



Corrosion Inhibition of Bronze Alloy by *Jatropha* Extract in Neutral Media for Application on Archaeological Bronze Artifacts

Almoatzbellah Elshahawi^{1*}, Mai Rifai¹, Zeinab Abdel Hamid^{2*}

¹ Conservation Department, Faculty of Archaeology, Cairo University

² Corrosion control and surface protection department, Central Metallurgical Research and Development Institute [CMRDI]



CrossMark

Abstract

Corrosion is a predominant problem for the different materials. Various methods have been utilized to prevent this phenomenon; some routes have caused great environmental effects, and are harmful to humans. Recently, green corrosion inhibitors have been used to overcome this problem. This paper discusses the corrosion inhibition behavior of bronze in 3.5% NaCl solution in the absence and presence of *Jatropha* extract as a green corrosion inhibitor. Bronze coupons were made based on the chemical composition of cast bronze alloys used in archaeological artifacts. The influence of inhibitor concentration and operating temperature on the inhibition efficiency was studied using weight loss, electrochemical techniques, salt spray, and colorimetric measurements. The results showed that *Jatropha* extract could serve as an effective inhibitor in 3.5% NaCl. The inhibition efficiency (IE%) increases with an increase in inhibitor's concentration but decreases with temperature rise. The highest inhibition efficiency was 90.36 % at 30 ppm of *Jatropha* and at room temperature [~ 25 °C]. The inhibition is attributed to the physical adsorption of the inhibitor on the surface of the bronze alloy. Finally, based on the findings of this study, *Jatropha* extract is highly recommended for use as a green corrosion inhibitor for archaeological artifacts.

Keywords: corrosion, inhibitor, bronze, *Jatropha*, green, artifacts.

1. Introduction

Bronze alloy has been used throughout history for the manufacture of various metal artifacts. Bronze objects from the Second Dynasty are known [Ogden 2000: 148-176]. Several well-known bronze objects from the Middle Kingdom are also present (about 2025-1700 BC). However, bronze wasn't widely used until the New Kingdom (about 1550-1069 BC) [Craddock 1995]. The main composition of the bronze alloy is copper and tin. The purpose of added tin is a high to increase the hardness and sharpness of the alloy. There are also other elements were mixed with copper, for example lead, arsenic, and antimony in order to make the alloy better able to resist corrosion, and increase the fluidity of the alloy to be easier to cast [Lechtman H. 1996: 477-514; Odler M. 2016: 238-257; Ingo G. M. et al. 2006: 513-520]. The melting temperature of the bronze is about 1,005 °C [Osterman V. and Antes H. 2010]. The bronze artifacts exposed in the indoor or outdoor environment often suffer from corrosion due to increasing atmospheric

pollution and non-adequate storage conditions [Rahmouni et al. 2009: 5206-5215]. The possibility of bronze corrosion prevention has attracted many researchers; so many inhibitors have been used to minimize the corrosion of bronze in different media. Corrosion inhibitors are the substance that, when applied to an environment in small quantities, effectively reduce the corrosion reaction [Miralrio et al. 2020: 1-27]. Particularly, organic compounds containing nitrogen, oxygen, and sulphur atoms are often used to protect bronze from corrosion. Unfortunately, most of these compounds are synthetic chemicals that may be very expensive and hazardous to living creatures and the environment [Muresan et al. 2007: 7770-7779]. Therefore, the development of non-toxic, ecologically harmless, natural corrosion inhibitors is regarded as a crucial alternative [Kusmierek et al. 2013: 169-174]. As a result, there is an increasing interest in natural inhibitors which are economic, safe, non-toxic, and environmentally friendly [Rani et al. 2010: 1-15]. Many researches in

*Corresponding authors: Almoatzbellah Elshahawi, (151088moatz@gmail.com) and Z. Abdel Hamid (forzeinab@yahoo.com)

Receive Date: 28 July 2022, Revise Date: 21 August 2022, Accept Date: 04 September 2022

DOI: 10.21608/EJCHEM.2022.149590.6622

©2022 National Information and Documentation Center (NIDO)

the field of metal protection focused on using natural plants extracts [Saidin et al. 2011: 5], such as the application of plant extracts as corrosion inhibitors for the protection of metal and its alloys from corrosion processes in different media [Radivojević et al. 2017: 1-22].

The purpose of this research is to investigate the efficiency of *Jatropha* extract as a green corrosion inhibitor for application on bronze archaeological artifacts in a neutral solution (3.5% NaCl) by using different techniques. Weight loss, electrochemical techniques, salt spray, and colorimetric measurements were used to estimate and investigate the corrosion rates and inhibition efficiency of *Jatropha* extract at different concentrations in neutral media.

2. Materials and Methods

For simulation experiments, quaternary bronze coupons were made based on the same chemical composition as archaeological cast bronze alloys (Cu-Sn-Zn-Pb) [Ingo G. M. et al. 2006; 513-520]. The chemical composition of the bronze coupons is illustrated in Table 1. The bronze coupons with dimensions 23x 33x6 mm were used during the test. The surface of the bronze coupons was prepared using emery paper of different grades up to 1200, and then, it was rinsed with triple distilled water. Oil, grease, and dirt were properly removed using an alkaline degreaser. After this stage, the specimen was rinsed in running water then in distilled water and finally kept in a desiccator to prevent atmospheric corrosion before experimentation. Tests were performed at different concentrations of *Jatropha* extract and different temperature (25, 35, and 45 °C ±1).

Table 1 Chemical composition of bronze alloy

Fe	Pb	Zn	Sn	Cu	Element
0.5	2.1	2.2	5.14	87.8	Wt. %

Corrosive Solutions and Corrosion Inhibitor

All experiments were carried out in 3.5% NaCl (POCH SA, Poland) solutions prepared using triply distilled water. Cold-Pressed *Jatropha* plant derivative was obtained from the "Unit of Oil Extracting and Pressing" at the National Research Centre, Egypt.

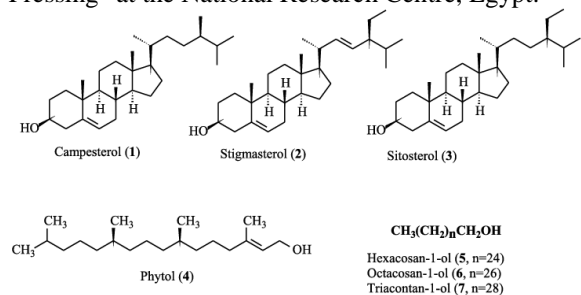


Fig. 1 Chemical structure of *Jatropha* plant derivative [Ribeiro S. S. et al. 2012].

Procedures used for corrosion measurements

Corrosion is an electrochemical process; electrochemical methods are the preferred analysis methods to study the corrosion behaviour of metals

[Letardi 2021: 1-16].

Potentiodynamic polarization (PDP)

Electrochemical studies were achieved using IviumStat instrument (supplied by Ivium technologies, Eindhoven, the Netherlands). The IviumStat software Different concentrations of *Jatropha* extract (10, 20, 30, 40, and 50 ppm). The chemical structure of *Jatropha* plant derivative is shown in Fig. 1. The selected inhibitor was applied to the surface of the bronze coupons by brushing.

The IviumStat software can be used to control IviumStat instrument with a personal computer (PC). The PC is used to specify the parameters of the measurement and to calculate the results of the measurements. A three-electrode cell system was utilized for the measurement; bronze alloy with an exposed area of 1.0 cm² is the working electrode (WE), whereas platinum sheet, and saturated calomel electrode (Hg/Hg₂Cl₂/Cl⁻) act as a counter electrode and reference electrode (SCE), respectively. Polarization experiments were measured after exposure the samples for 1 h to the test solution. All polarization curves were performed in 3.5% NaCl solutions with and without the addition of different inhibitor concentrations, and the electrodes were immersed in the test solution at the natural potential to attain the steady state before the measurement. The potentiodynamic current-potential curves were recorded by changing the electrode potential automatically from - 0.50 to + 0.50V (SCE) and at a scan rate of 0.5 mVs⁻¹. Tafel plots were illustrated by plotting E vs log I. Corrosion potential (E_{corr}), corrosion current densities (I_{corr}), polarization resistance (R_p), cathodic and anodic slopes (β_c and β_a) were calculated according to the well-known procedures. The inhibition efficiency (IE%) was calculated using the following equation 1:

$$IE \% = \frac{I'_{corr} - I_{corr}}{I_{corr}} \times 100 \quad (1)$$

Where; I'_{corr} and I_{corr} are the corrosion current density without and with the inhibitor, respectively.

Electrochemical Impedance Spectroscopy (EIS)

EIS was carried out at the corrosion potential (E_{corr}) with a frequency ranging from 0.1 to 60000 Hz at an amplitude of 5 mV. The impedance diagrams are given in the Nyquist and bode plot representation. The IE% was calculated from the charge transfer resistance (R_{ct}) values which were obtained by subtracting the high-frequency impedance using the following equation 2. The degree of surface coverage (θ) was calculated using Equation 3.

$$IE \% = \frac{R_{ct}(in) - R_{ct}(un)}{R_{ct}(in)} \times 100 \quad (2)$$

$$\theta = \frac{IE}{100} \quad (3)$$

Where; R_{ct}(in) and R_{ct}(un) are the charge transfer resistance of bronze alloy with and without the inhibitor, respectively.

Weight loss measurement

Weight loss (WL) represents the simplest, common, and classical technique for calculating the average corrosion rate (CR). This technique is based on the mass lost by corrosion, which is directly monitored to obtain the corrosion rate. In this method, the weight variations of the metal sample are calculated before and after exposure to the corrosive medium in the absence and presence of inhibitor. A corrosive solution of 3.5% NaCl was prepared by dilution in distilled water. The corrosion rate was assessed at room temperature and different concentrations of *Jatropha* extract (10, 20, 30, 40, and 50 ppm). Uninhibited and inhibited bronze coupons were exposure to the test solution of 3.5% NaCl in the presence and absence of the *Jatropha* extract. The specimens were withdrawn from the test solutions after 72hrs at room temperature 25 ± 1 °C. The weight loss was calculated as the difference in weight of the specimens before and after immersion, determined using a digital balance (Uni Bloc ux2200H) with a sensitivity of ± 1 mg. The inhibition efficiency and degree of surface coverage (θ) were calculated using equations 4 and 5, respectively.

$$IE \% = \frac{W_1 - W_2}{W_1} \times 100 \quad (4)$$

$$\theta = \frac{W_1 - W_2}{W_1} \quad (5)$$

Where; W_1 and W_2 are the weight loss in the absence and presence of the inhibitor, respectively.

Salt Spray Test

Salt spray testing is one of the most common corrosion evaluation tests for protective coatings and inhibitors metals. It is used to compare different inhibited substrates to each other or to uninhibited substrates [Pajkossy 1994: 111-125; Abdel Hamid et al. 2016: 38-49]. Salt fog testing exposes substrates to a humid, salt depositing, corrosive atmosphere and monitors any resulting deterioration of the surface. The appearance of corrosion on the surface is the criterion used to determine the level of protection. Neutral salt spray test was performed according to ASTM B117 standard using Ascott cabinet (CC1000ip). Salt spray test was used to investigate the corrosion behaviour of bronze samples inhibited and uninhibited with different concentrations of *Jatropha* extract in 5% NaCl electrolyte at 35 °C. The objective of this experiment was to determine whether *Jatropha* extract would provide corrosion protection under salt fog conditions and to predict its suitability in use as a protective finish [Usman et al. 2020: 1:16]. The appearance of corrosion products is evaluated after a pre-determined time. Test duration depends on the corrosion resistance of the inhibitor [ASTM B117 2021; Barth 2008: 1-9; Winnicki et al 2017: 1935–1946; Sastri et al. 2007: 80-90].

Colorimetric measurements

Reflectance measurement is a useful parameter for the quantitative evaluation of the

aesthetic appearance of corrosion inhibitors for archaeological bronze artifacts [Albini 2017: 90; Sastri et. 2011: 257–288; Franceschi et al. 2006: 166–170]. It's a non-destructive test and it has an important parameter for cultural heritage applications. Color measurements were determined according to European Standard EN 15886 (European Committee for Standardization 2010) with a portable KONICA MINOLTA CM2600D spectrophotometer in SCI/SCE mode with d/8 configuration provided with Spectra Magic 3.5 software has been used to obtain reflectance measurements in the range 400–700 nm. To follow the evolution of the aesthetic appearance through the different surface treatments, three equally spaced measuring points along one diagonal were selected for each coupon and localized using a transparent paper sheet. On the test coupons, 12 evenly spaced points were selected. Calibration was made with a white calibration plate CM-A415 (Minolta). On each bronze coupon (2.3 cm \times 3.2 cm \times 0.6 mm). Special care is required when measuring inhibited coupons, as the target mask could damage their soft surface. Although SCE is used for measurements on metallic surfaces, both SCI and SCE results are displayed for comparative purposes.

The colorimetric data of the coupons were calculated from the acquired spectra according to the CIEL*a*b* colour space for each selected point (O~8 mm) after each treatment step (sandblasting and inhibiting). According to this color representation L^* is lightness, a^* is the red-green component, b^* is the yellow-blue component. In the CIEL*a*b* system, the distance between any two color points represents their color difference (ΔE^*) and it is calculated from the differences of its component ΔL^* , Δa^* , and Δb^* as shown in equation 6 [Bacci et al. 1997: 28; Siatou et al. 2007: 1-6; Chang 2018: 36; Cecchel et al. 2018: 70-78].

$$\Delta E = \sqrt{(\Delta L^*)^2 + (\Delta a^*)^2 + (\Delta b^*)^2} \quad (6)$$

The colorimetric difference equation was originally designed for the calculation of small differences ($\Delta E < 10$). Higher values will be considered for comparative purposes [Graziani et al. 2014: 193-203]. Total color change (ΔE^*) in the range between 3 and 5 is generally considered acceptable in the field of cultural heritage (not perceptible to the human eye), while values lower than 3 are considered while ΔE^* bigger than 5 are considered perceptible [Letardi et al. 2002; 22-27; Letardi 2002: 272-275].

In this study, colorimetric measurements were performed for blank coupons, then after coating with different concentrations of *Jatropha* extract, and finally after subjecting to artificial weathering using UV light for 21 days. The color sampling tool was used for each coupon to obtain average $L^*a^*b^*$ values from three zones and to compare the colorimetric data. The variation in colour difference ΔE was performed between the blank coupons and the ones coated with

Table 2. Tafel polarization parameter values for the corrosion of the bronze alloy electrode without and with different concentrations of *Jatropha* in 3.5% NaCl solution

Conc, ppm	E_{corr} , V	I_{corr} , A/cm ²	R_p , Ω	β_a , V/dec	β_c , V/dec	C. Rate, mm/y	IE %	θ
Blank	-0.2005	3.339E-6	2856	0.114	0.071	0.03871	-----	-----
10	-0.2442	1.184E-6	7380	0.068	0.099	0.0137	64.54	0.6454
20	-0.251	1.012E-6	6635	0.054	0.072	0.01173	69.69	0.6969
30	-0.2000	4.626E-7	9033	0.036	0.041	0.00536	86.14	0.8614
40	-0.2721	1.086E-6	5934	0.055	0.064	0.0126	67.47	0.6747
50	-0.1814	1.306E-6	4436	0.066	0.045	0.01515	60.88	0.6088

Jatropha, and those subjected to artificial weathering [Letardi 2002: 1-16; Sathiyabama et al. 2006: 363-370].

Results and Discussion

Electrochemical Considerations

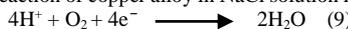
Potentiodynamic Polarization Considerations

The polarization curves of the bronze electrode immersed in 3.5% NaCl without and with the addition of different concentrations of inhibitor operated at ambient temperature (25 °C) are illustrated in Fig. 2. The electrochemical parameters such as the corrosion potential (E_{corr}), the corrosion current density (I_{corr}), polarization resistance (R_p), anodic (β_a), and cathodic (β_c) Tafel slopes are summarized in Table 2. Anodic and cathodic polarization curves were recorded to obtain information about the effect of the inhibitor on the corrosion processes. It was observed that in every curve in the presence of the inhibitor I_{corr} changed towards lower values compared with that in the absence of the inhibitor. The results indicated that the presence of *Jatropha* plant extractor compounds reduced anodic dissolution and also retarded the hydrogen evolution reaction. The IE% was evaluated and the results proved that IE % of the inhibitor increases with increasing its concentrations. No clear trend was observed in the shift of E_{corr} values in the presence of various concentrations of inhibitor, suggesting that this compound behaves as a mixed-type inhibitor [Fouda et al. 2016: 1-15]. The role of *Jatropha* plant extraction in decreasing the corrosion rate could be due to the presence of hetero-atoms and π -electrons in the *Jatropha* plant extraction compounds for making adsorption; it may act as an adsorption inhibitor. The inhibitor controlled the anodic and cathodic reactions during the corrosion process; therefore, its corrosion inhibition efficiency is directly proportional to the amount of adsorbed inhibitor up to 30 ppm concentration. So, the structure of the inhibitor plays an important role during the adsorption process. On the other hand, an electron transfer may take place during adsorption of the organic compounds on the metal surface. Corrosion rate is usually controlled by the cathodic and anodic

reactions. The anodic reactions of copper alloy in the NaCl solution are:



The cathodic reaction of copper alloy in NaCl solution is as follows:



The total copper corrosion reaction in NaCl solution is:



When solid copper dissolves, copper ions chelate with Cl^- the existence of Cl^- ions subsequently speeds up the dissolution of copper (Sangeetha et al. 2011).

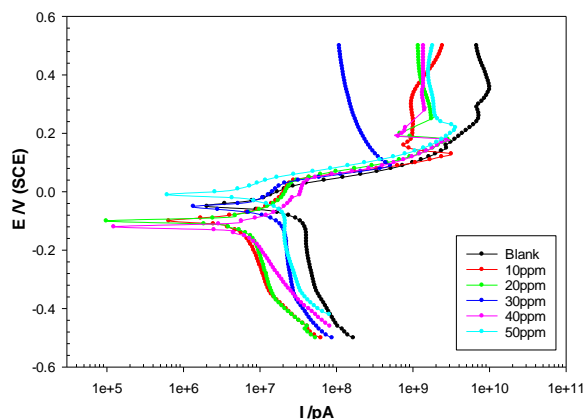


Fig. 2 Polarization curves of bronze electrodes without and with *Jatropha* extract at different concentrations in 3.5% NaCl solution

From Table 2 and Fig. 2, the results reveal that E_{corr} of the copper alloy electrode when immersed in the 3.5 %NaCl solution is -0.2005V, and I_{corr} is 3.339E-6 A/cm². While, these values decreased when the copper alloy electrode was immersed in the NaCl solution containing *Jatropha*. As a result, *Jatropha* molecules could inhibit Cl^- from corroding copper alloy. The opportunity for Cl^- to make contact with the surface decreases, thereby effectively inhibiting copper dissolution in the anode. IE% increases with increasing *Jatropha* concentration as shown in Table 2. The highest IE% is about 86.14% in the coupons inhibited with 30 ppm of *Jatropha* extract. The IE% decreased after increasing the concentration above 30ppm as shown in Table 2 [Sangeetha et al. 2011: 275-280].

Electrochemical Impedance Spectroscopy (EIS) Considerations

EIS technique was applied to investigate the electrode/electrolyte interface and corrosion processes that occur on the bronze alloy surface in the presence and absence of *Jatropha* plant extraction molecules in the electrolyte. The impedance spectra of bronze alloy immersed in 3.5% NaCl aqueous solution in the absence and presence of inhibitor operated at room temperature are shown in the form of Nyquist plots in Fig. 3a and Bode plots in Fig. 3b. The impedance $\log(Z/\Omega)$ values are derived from Bode plots. Using Ivium software, the impedance spectra of the different Nyquist plots were analysed by fitting the experimental data to a simple equivalent circuit model. It was found that the equivalent circuit that fit the experimental data consists of either one time constant model $R_s(R_{ct}C_{dl})$ or $R_s(R_{ct}C_{dl}W)$ for bronze alloy electrodes in NaCl solutions with and without inhibitor as given in Fig. 4.

The circuit one includes the solution resistance (R_s), double layer capacitance (C_{dl}), and the charge transfer resistance (R_{ct}), while circuit two includes Warburg impedance (W). The data reveals that each impedance diagram consists of a large capacitive loop with low frequencies dispersion. It can be seen that, when bronze alloy immersed in the aqueous 3.5% NaCl solution containing 30 ppm inhibitor the R_{ct} value increases from $1.056E+03$ to $1.069E+04$ Ohm, and the C_{dl} value decreases from $1.322E-04$ to $2.033E-05$ μFcm^{-2} .

The increase of R_{ct} and the decreasing of the C_{dl} with the increase of the inhibitor concentration may be due to the increase in the surface coverage by the inhibitor molecules [Kesavan et al. 2012: 1-8]. The foregoing results can be explained because the inhibitor adsorption on the bronze surface produces a physically protective barrier that hinders the process of charge transfer and hence slows corrosion reactions and causes R_{ct} value to rise. As the diameter of the Nyquist plot grows, the corrosion rate decreases with increasing inhibitor concentration. Furthermore, the adsorbed inhibitor species reduces the electrical capacity of the electrical double layer at the electrode/solution interface, lowering C_{dl} values [Rani et al. 2012: 1-15].

Table 3 also includes the calculated IE% values for different concentrations of this inhibitor at room temperature. Rct values were used to calculate the IE%. The corrosion rate is proportional to the reciprocal of charge transfer resistance ($1/R_{ct}$). The values demonstrated that the IE% increases as the inhibitor concentration increases.

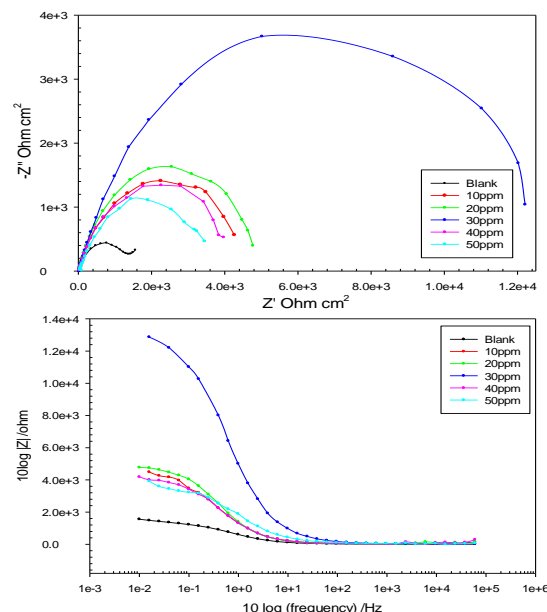


Fig. 3 EIS of bronze electrode in different concentrations of *Jatropha* extract. 3.5% NaCl solution at ambient temperature. (a) Nyquist plot and (b) Bode plots

From Fig. 3 (a), a small capacitive loop in the high-frequency region, and a straight line (Warburg) in the low-frequency area are observed in the Nyquist plots of the bare bronze alloy electrode without inhibitor. The capacitive loop is attributed to the R_{ct} , whereas the Warburg impedance is attributed to the diffusion of the anodic and cathodic reaction products from the solution to the electrode surface [Popoola 2019: 71-102; Rani et al. 2010: 58-64; Rani et al. 2011: 38-49; Zaferani et al. 2013: 652-657].

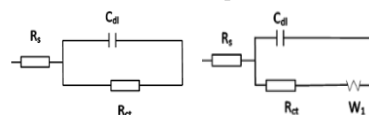


Fig. 4 The equivalent electrical circuit model (measured and fitted Nyquist plots).

Moreover, the results of Fig. 3 illustrated that R_{ct} increases after the electrode surface is inhibited by *Jatropha* extract films. The arc radius increases with increasing *Jatropha* concentration, which signifies increased R_{ct} values. IE % is calculated from equation 2 and the results reveal that the IE % increases with increasing *Jatropha* concentration. The highest IE % value is 90.36 % at 30 ppm. The increased charge transfer resistance is related to the self-assembled films. Therefore, *Jatropha* extract can inhibit the corrosion of bronze in 3.5% NaCl solution.

Temperature effect considerations

Because various changes on the metal surface, such as rapid etching and desorption of inhibitor, as well as breakdown and/or rearrangement

of the inhibitor, the influence of temperature on the inhibited solution–metal reaction is highly complex. The influence of temperature was applied to investigate the inhibition efficiency and the adsorption

process that occur on the bronze alloy surface in the presence and absence of optimum molecules concentration of *Jatropha* extract in the electrolyte.

Table 3 Impedance parameters for bronze electrodes without and with *Jatropha* inhibitor at different concentrations in 3.5% NaCl solution operated at room temperature

Conc. ppm	R _s Ω cm ²	R _{ct} Ω cm ²	C _{dl} , μF cm ²	W1/ (Ω sqrt (Hz))	IE%	θ
Blank	4.989E+01	1.056E+03	1.322E-04	1.072E+02	-----	-----
10	2.038E+02	3.877E+03	9.727E-05	-----	72.76	0.7276
20	1.343E+02	4.286E+03	8.002E-05	-----	75.36	0.7536
30	4.483E+02	1.096E+04	2.033E-05	-----	90.36	0.9036
40	1.763E+02	3.602E+03	8.930E-05	-----	70.68	0.7068
50	1.654E+02	3.135E+03	4.632E-05	-----	66.31	0.6631

Table 4. Impedance parameters for bronze electrode without and with optimum concentration of *Jatropha* extract at different temperatures in 3.5% NaCl solution

Temp. °C	Conc. ppm	R _s Ω cm ²	R _{ct} Ω cm ²	C _{dl} , μF cm ²	W1/ (Ω sqrt (Hz))	IE%	θ
25	0	4.989E+01	1.056E+03	1.322E-04	1.322E-04	-----	-----
	30	4.483E+02	1.096E+04	2.033E-05	----	90.36	0.9036
35	0	3.500E+01	6.409E+02	1.292E-04	9.619E+01	-----	-----
	30	5.626E+01	1.188E+03	7.767E-05	1.210E+02	46.05	0.4605
40	0	2.728E+01	2.888E+02	1.647E-04	5.218E+01	-----	-----
	30	5.142E+01	4.544E+02	1.017E-04	6.995E+01	36.44	0.3644
45	0	2.340E+01	4.675E+02	1.357E-04	8.773E+01	-----	-----
	30	7.530E+01	6.695E+02	1.210E-04	1.007E+02	31.17	0.3117

Adsorption Isotherm

Adsorption isotherms explain the mechanism of adsorption as well as the interplay between metal surfaces and inhibitor molecules. The data from the EIS study were graphically fitted into various isotherms (Langmuir (C versus C/θ), Freundlich (C versus θ), and Temkin (C versus log θ) adsorption isotherms) as shown in Fig. 5(a-c). The extent of surface coverage in the different concentrations of *Jatropha* leaves extract helps

The impedance spectra of bronze alloy immersed in 3.5% NaCl aqueous solution in the absence and presence of 30ppm inhibitor concentration operated at different temperatures are shown in Table 4. The results show that the temperature impact is more pronounced on the overall corrosion reaction. With the increase in temperature, the efficiency of the inhibitor was reduced. The results have demonstrated the R_{ct} value decreases from 1.096E+04 Ohm cm² to 6.695E+02, and the C_{dl} value increases from 2.033E-05 to 1.210E-04 μF cm². A decrease in effectiveness with an increase in temperature usually means that the corrosion inhibitor is physisorbed.

The extent of surface coverage in the different concentrations of *Jatropha* extract helps to determine the isothermal best matched for the studies

by assessing the coefficients of correlation in the isotherms. From Fig. 5 straight line of C/θ versus C plots (Fig. 5a) indicate that the adsorption of the inhibitor molecules on the metal surface obeyed Langmuir adsorption model, and the linear regression coefficient (R²) is almost equal to 1 (Langmuir

isotherm has the best correlation coefficients (R²) compared with the other isotherms. The Langmuir isotherm was found to be suitable for the experimental results. It is the most basic and is based on the assumption that all adsorption sites are equal and particle binding occurs independently of surrounding sites [Fabjan et al. 2011, 585–591]. Langmuir isotherm is described by the following equation (11) and K_{ads} value (the equilibrium constant of adsorption process) can be calculated from the intercepts of the straight lines on the C/θ-axis.

$$\frac{C}{\theta} = \frac{1}{K_{ads}} + C. \quad (11)$$

Where C is the inhibitor concentration, K_{ads} is the equilibrium constant of adsorption process, θ is the degree of surface coverage.

The substitution adsorption process between the inhibitor molecules (Inh_(sol)) and the water molecules on the metal surface is described as inhibitor adsorption at the metal/solution interface (H₂O_{ads}):



Where Inh_(sol) and Inh_(ads) are the inhibitor species that have been dissolved in aqueous solution and adsorbed onto the metal surface, respectively. The quantity of water molecules adsorbed on the metal surface is denoted by H₂O_{ads}, and the number of water molecules replaced by a single inhibitor molecule is denoted by x. The type of metal, the nature of the metal's surface, the nature of the corrosive medium, the pH value, the temperature, and the electrochemical potential of the metal – solution interface all influence adsorption. Adsorption also reveals information on the

interactions of the adsorbed molecules with one another and with the metal surface. Physical adsorption and chemisorption are two forms of interactions that describe the adsorption of an organic component. The calculated values for E_a parameter for the corrosion reaction to illustrate the nature of adsorption were calculated using an Arrhenius equation (13):

$$\ln(k_2/k_1) = E_a/R \times (1/T_1 - 1/T_2) \quad (13)$$

where;

E_a = the activation energy of the reaction in J/mol

R = the ideal gas constant = 8.3145 J/K·mol

T_1 and T_2 = absolute temperatures (in Kelvin)

k_1 and k_2 = the reaction rate constants at T_1 and T_2

Table 5 Corrosion parameters of bronze coated with various concentrations of *Jatropha* extract after 72hrs in 3.5% NaCl

Inhibitor conc. ppm	Wt. _b immersion /g	Wt. _a immersion /g (b. washing)	After Immersion (after washing) /g	WL /g	Efficiency %	θ
Blank	42.9945	42.9977	42.9910	0.0035	-----	-----
10	40.3870	40.3874	40.3860	0.0010	71.42	0.7142
20	39.8142	39.8144	39.8134	0.0008	77.14	0.7428
30	43.2059	43.2065	43.2057	0.0002	94.28	0.9428
40	44.1185	45.1184	45.1176	0.0009	74.28	0.7714
50	40.8680	40.8585	40.8567	0.0013	62.85	0.6285

The results calculated that the E_a of the blank is 63.35 KJ/mol while the E_a of the inhibited solution is 238.6 KJ/mol. Increased E_a in the inhibited solutions compared to that in blank suggests that the inhibitor is physically adsorbed on the corroding metal surface. Generally, increased E_a in the inhibited solutions suggests that the inhibitor is physically adsorbed on the metal surface while either unchanged or lower E_a in the presence of inhibitor suggest chemisorptions [Tang et al. 2010: 101-105].

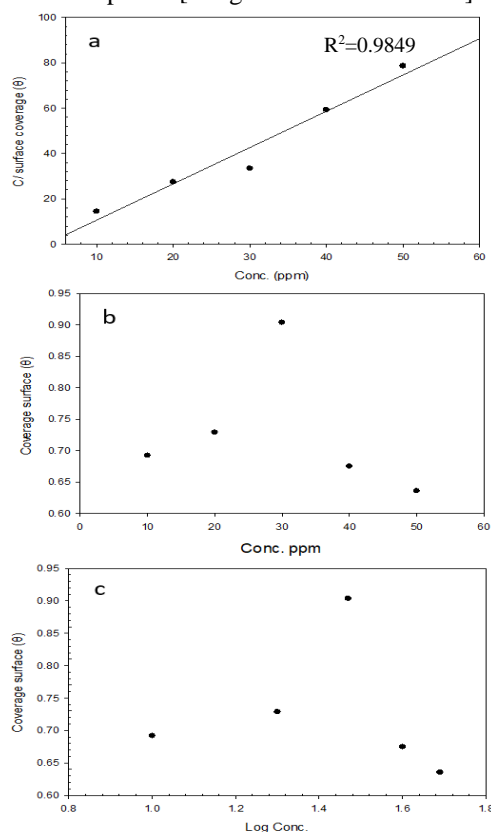


Fig. 5 Different adsorption isotherms of *Jatropha* plant extraction on bronze surface in 3.5 % NaCl at 25 °C, where, a) Langmuir, b) Freundlich, and c) Temkin adsorption isotherms.

Weight Loss considerations

The weight loss technique was employed as a chemical testing technique to evaluate the influence of inhibitor compounds at different concentrations on the corrosion of bronze in 3.5% NaCl for 72hrs at room temperature. The corrosion behavior of bronze is characterized by measuring the weight loss of a specimen before and after exposure to corrosive media. The results of this method are summarized in Table 5, as shown a remarkable increasing in IE% was observed with increasing concentration indicates that the well coverage of the inhibitor onto the bronze surface. The change in the weight of inhibited samples was negligible in comparison with the uninhibited samples, which increased in weight by 0.0035% this suggests a continuation of the active corrosion processes in the alloy of the uninhibited samples. Moreover, the surface coverage (θ) is increased with an increase of inhibitor concentration from 10 to 30ppm.

Salt Spray considerations

The salt spray test is a standardized and popular corrosion test method, used to check corrosion resistance of materials. Salt spray testing helps compare different coatings' protective properties relative to each other when tested under the same conditions. Tested bronze coupons are placed in an enclosed salt spray testing cabinet and subjected to a continuous indirect fog of a salt water solution. The IS series standard salt spray test chamber from Ascott analytical was used for this experiment.

Parameters of testing:

- temperature in the salt-spray chamber 35 ± 2 °C, and 90% for relative humidity
- concentration of the sodium chloride in a spraying medium 5 wt.% NaCl solution
- pH value of the salt solution 6.5–7.2,
- time interval was set for 1, 2, and 3 days.

The maximum of 88.57% inhibition efficiency is observed at a higher

concentration (30 ppm) of *Jatropha* extract as shown in table 5.

The results are given rather in qualitative than quantitative form. The salt fog test results show that a small concentration of *Jatropha* extract can protect bronze coupons from corrosion created by harsh, salt fog environments. Results of the salt spray test as shown in Table 6,7 and Fig 6. reveal that after 72hrs holding time according to B117 ASTM, no corrosion appeared on the surface inhibited with 30ppm

inhibitor, indicating a good corrosion resistance at this concentration. Results showed that the samples coated with rust converter provide a good significant protection against corrosion phenomenon than the uninhibited samples (blank) with *Jatropha* extract. Thicker inhibiting layers can help provide additional protection and help ensure coverage of the surface of the bronze substrates.

Table 6 the relative resistance to corrosion of bronze coupons inhibited by different concentration of *Jatropha* extract exposed to sodium chloride salt spray climate at 35°c

Media/ Condition	Concentration / ppm	Observations
NaCl 5% at 72 hrs at 35 °c	Different concentration of <i>Jatropha</i> (10 to 50 ppm)	The concentrations 10, 20, and 30 ppm showed a good corrosion resistance to the salt spray test where is a bit of change; but the concentrations 40, 50 ppm were showed a low corrosion resistance and a big change in the surface appearance and different colors of corrosion products were formed on the surface of the coupons as well

Table 7 Results of salt spray test on bronze coupons inhibited by *Jatropha* extract

Concentration	Test time		
	after 24 hrs	after 48 hrs	after 72 hrs
Blank	O	✓	✓
10	□	O	✓
20	□	O	O
30	□	O	O
40	□	✓	✓
50	O	✓	✓

□: Normal
O: Corrosion started
✓: Corrosion

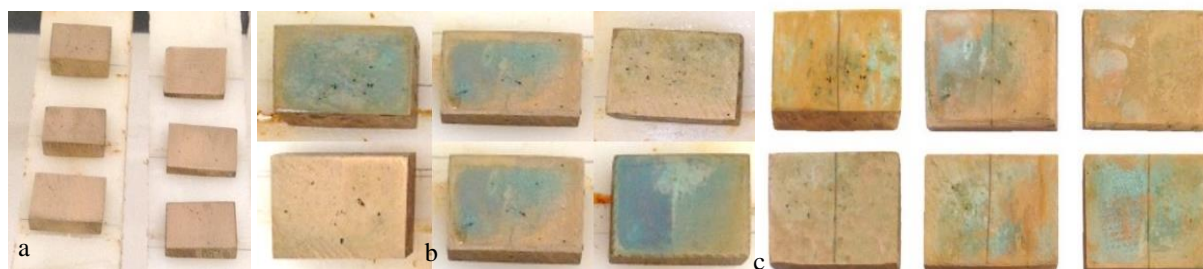


Fig. 6 bronze coupons (a) before (b, c) after exposure to salt spray test

Colorimetric measurement considerations

As the aesthetic properties are one of the most important features of the application of corrosion inhibitors on the surface of metal artifacts, colorimetry tests were performed in order to measure the color differences between the inhibited and uninhibited bronze coupons using a Konica Minolta CM-700d spectrophotometer.

Twelve points evenly distributed on the surface were measured in the blank coupons and in the inhibited coupons with *Jatropha* extract. The colorimetric results are reported in CIE L*a*b* color space. Both SCE and SCI color measurement values performed on blank bronze coupons and those inhibited with *Jatropha* extract are reported in Table 8.

The inhibitor did not change the color in a perceivable way. Higher values of SCI are linked to their glossy appearance. The a* (red-green component) and b*(yellow-blue component) values for all blank and inhibited coupons are almost similar.

ΔE average behaviour for inhibited coupons exposed to UV radiation after 21 days is displayed in Table 9. The Δa^* values for all weathered coupons are almost similar. A little more variation upon weathering is observed for Δb^* . The L* values are the more subject to UV radiation, and the ΔE behaviour is shown in Table 9 is mainly due to ΔL^* . Conversely, the inhibited sample showed a slight color variation ($\Delta E^* < 5$), indicating no appreciable visual alteration of the inhibitor due to accelerated aging.

Table 8. Average and standard deviation of CIE L*a*b* colorimetry results for bronze coupons

Sample	SCI			SCE		
	L*	a*	b*	L*	a*	b*
Blank	81.85 (± 2)	5.21 (± 02)	14.65 (± 1)	68.47 (± 2)	4.22 (± 03)	12.33 (± 09)
Jat. 30 ppm	78.74 (± 1)	7.49 (± 07)	19.31 (±09)	69.82 (±3)	7.15 (±02)	18.68 (±06)

Table 9. Average behaviour of colour difference (ΔE) on the test coupons inhibited with *Jatropha* extract after exposure to UV radiation for 21 days.

	SCI				SCE			
	ΔL	Δa	Δb	ΔE	ΔL	Δa	Δb	ΔE
Jat. 30 ppm	-3.11 (± 2)	2.28 (± 03)	4.66 (± 05)	5.36 (± 2)	1.35 (± 2)	2.93 (± 05)	6.35 (± 04)	4.54 (± 1)

Application to archaeological bronze artifacts

Experimental studies examining the use of *Jatropha* extract as a green corrosion inhibitor for the corrosion protection of bronze coupons revealed that *Jatropha* extract can be used and applied as a corrosion inhibitor in protecting an ancient Egyptian bronze mirror stored in the Grand Egyptian Museum, Conservation Center (GEM-CC). 30ppm *Jatropha* extract was applied on both sides of the mirror in three intersecting layers, with 10ppm silver nanocomposites added to strengthen the inhibitor's characteristics and due to silver particles' anti-fungal activities (Fig. 7).



Fig. 7 the bronze mirror before and during conservation (a) and after conservation and applied the optimum concentration of *Jatropha* extract on the mirror's surfaces (b, c)

Conclusion

The following conclusions can be drawn from our present study:

- The *Jatropha* extract acts as an effective and efficient inhibitor for the bronze alloy in 3.5% NaCl.
- The inhibition efficiency increased with the increase of inhibitor concentration to reach the maximum of 90.36% at 30 ppm of the extract but decreased with increasing temperature.
- The inhibition is attributed to the physical adsorption of the inhibitor on the surface of the bronze coupons.
- In the classic weight reduction rate, the inhibition efficiency of *Jatropha* extract was determined to be 94.28%.
- The difference between SCE and SCI colour value can be easily used as a parameter to quantify the matt-gloss appearance of Inhibitors, which is a relevant factor in the selection of an aesthetically acceptable protective treatment for archaeological bronze artifacts.

- Based on the colorimetric experiments performed, *Jatropha* extract didn't change the appearance and aesthetic of bronze coupons and the color change is in the standard range. The extract shows a good appearance of the original surface of the bronze coupons. The difference in color ΔE is low < 5. Therefore, the differences between the inhibited and uninhibited bronze coupons are unnoticeable.
- This study recommends the use of *Jatropha* extract as a green corrosion inhibitor for application on archaeological artifacts.

Acknowledgements

The authors would like to express their gratitude to Dr. Mona Hassan and Mr. Yehia Makhlof, Corrosion Control and Surface Protection Department, CMRDI, for their unwavering support.

References

1. Abdel Hamid Z, Helal AM, Atia AM, Megahed HE (2016) Performance of Morus Alba Plant Derivative as Corrosion Inhibition of Mild Steel in HCl Solution. *Journal of Metallurgical Engineering* 5:38–49
2. Albin M (2017) Fungal biogenic patina: optimization of an innovative conservation treatment for copper-based artefacts. Ph.D dissertation, University of Neuchâtel, Faculty of Science, Laboratory of Technologies for Heritage Materials and Laboratory of Microbiology:99
3. ASTM B117 (2021) Standard Method of Salt Spray (Fog) Testing. ASTM International, West Conshohocken, PA: <http://www.astm.org/Standards/B117>
4. Bacci M, Picollo M, Porcinai S, Radicati B (1997) Non-destructive spectrophotometry and colour measurements applied to the study of works of art. *Mater Tech*:5-28
5. Barth D (2008) A Corrosion Analysis of Aluminum Alloys and Coatings. *BetaLED*:1–9
6. Cecchel S, Cornacchia G, and Gelfi M (2018) A study of a non-conventional evaluation of results from salt spray test of aluminum High Pressure Die Casting alloys for automotive components. *materials and corrosion*:70–78
7. Chang T (2018) Atmospheric corrosion of copper and copper-based alloys in architecture. Ph.D thesis, KTH Royal Institute of Technology, Department of Chemistry, Division of Surface and Corrosion Science, Stockholm, Sweden: 35
8. Paul T. Craddock. (1995). *Early Metal Mining and Production*. Edingburgh.
9. Ekanem UF, Umoren SA, Udusoro II, Udoh, AP (2010) Inhibition of mild steel corrosion in HCl using pineapple leaves (*Ananas comosus* L.) extract. *Journal of Materials Science* 45:5558–5566

10. Elia A (2013) Application of electrochemical methods for the study and protection of heritage copper alloys. Ph.D Thesis, Ghent University:53–56
11. Fabjan ES, Kosec T, Kuhar V, Legat A (2011) Corrosion Stability of Different Bronzes in Simulated Urban Rain Mater. Tech 45:585–591
12. Fouda AS, and Fouad RR (2016) New azonitrile derivatives as corrosion inhibitors for copper in nitric acid solution. Cogent Chemistry, Volume 2:1-15
13. Franceschi E, Letardi P, Luciano G (2006) Colour measurements on patinas and coating system for outdoor bronze monuments. Journal of Cultural Heritage 7:166–170
14. Graziani L, Quagliarini E, Bondioli F, and D’Orazio M (2014) Durability of self-cleaning TiO₂ coatings on fired clay brick facades: Effects of UV exposure and wet & dry cycles. Building and Environment 71:193–203
15. Ingo G. M., et al. (2006) Large scale investigation of chemical composition, structure and corrosion mechanism of bronze archeological artefacts from Mediterranean basin. Applied Physics A – Materials Science & Processing A 83: 513–520.
16. Kesavan D, Gopiraman M, Sulochana N (2012) Green Inhibitors for Corrosion of Metals: A Review. Che Sci Rev Lett, 1(1):1–8
17. Kusmierek E, and Chrzescijanska E (2013) Tannic acid as corrosion inhibitor for metals and alloys. Mater. Corros. 66, Issue 2:169-174
18. Lechtman, H (1996) Arsenic Bronze: Dirty Copper or Chosen Alloy? A View from the Americas,” Journal of Field Archaeology 23, no. 4 (Winter 1996): 477–514.
19. Letardi P (2004) Patinas and protective coating systems for outdoor bronze Monuments. Laboratory and field test on in: J. Ashton, D. Hallam (Eds.) Proceedings of the International Conference on Metals Conservation, National Museum of Australia:379–387
20. Letardi P (2021) Testing New Coatings for Outdoor Bronze Monuments: A Methodological Overview. coatings 11:1–16
21. Letardi P, Cozzolino D (2002) Contact-probe EIS characterisation of protective coating systems for outdoor bronze sculpture: atmospheric weathering behaviour in marine environment. in: International Corrosion Council (Eds), Proceedings of 15th International Corrosion Congress, Frontiers in Corrosion Science and Technology, Granada: 22–27
22. Letardi P, Marabelli M, D’Ercoli G, Guida G (2002) Comparative study of Protective Coating Systems for outdoor bronze sculpture. in: A. Guarino (Ed.), Proceedings of Third International Congress on Science and Technology for the Safeguard of Cultural Heritage in the Mediterranean Basin, CNR, Rome:272–275
23. Miralrio A, Vázquez AE. (2020) Plant Extracts as Green Corrosion Inhibitors for Different Metal Surfaces and Corrosive Media: A Review. Processes:1–27
24. Muresan L, Varvara S, Stupnisek-Lisac E, Otmacic H, Marusic K, Horvat-Kurbegovic S, Robbiola L, Rahmouni K, Takenouti H (2007) Protection of bronze covered with patina by innocuous organic substances. Electrochimica Acta 52:7770–7779
25. Odler, M. (2016) Old Kingdom Copper Tools and Model Tools. Archaeopress and Faculty of Arts, Charles University, Czech Institute of Egyptology: 238-257.
26. Ogden, J. (2009) Metals, in Ancient Egyptian Materials and Technology, ed. Paul T. Nicholson and Ian Shaw, Cambridge: Cambridge University Press: 148–76.
27. Osterman V. and Antes H. (2010) Critical Melting Points and Reference Data for Vacuum Heat Treating. Solar Atmospheres Inc: 1-41.
28. Pajkossy, T. (1994) Impedance of rough capacitive electrodes. J. Electroanal. Chem. 364:111–125
29. Popoola Lk (2019) Organic green corrosion inhibitors (OGCIs): a critical review. Corros Rev. 37(2):71–102
30. Radivojević M, Pendić J, Srejić A, Korac M., Davey C, Benzonelli A, Martinón M, Jovanović N, and Kamberović Ž (2017) Experimental design of the Cu-As-Sn ternary colour diagram. UCL Institute of Archaeology:1–22
31. Rahmouni K, Takenouti H, Hajjaji N, Srhiri A, Robbiolac L (2009) Protection of ancient and historic bronzes by triazole derivatives. Electrochimica Acta 54:5206–5215
32. Rani BEA, and Basu, BBJ, (2012). Green Inhibitors for Corrosion Protection of Metals and Alloys: An Overview. Int. J. Corros.:1–15
33. Rani DP, Phil MM, and Selvaraj S (2011) Comparative Account of *Jatropha curcas* on Brass (Cu-40Zn) in Acid and Sea Water Environment. PJST 12, Number 1:38–49
34. Rani PD, and Selvaraj S (2010) Inhibitive and Adsorption Properties of Punica Granatum Extract on Brass in Acid Media. J. Phytol. 2/11:58–64
35. Rani, D. P., and Selvaraj, S., 2010, "Inhibitive and Adsorption Properties of Punica Granatum Extract on Brass in Acid Media", J. Phytol.: 58–64
36. Ribeiro S. S. et al. (2012) Chemical Constituents of Methanolic Extracts of *Jatropha Curcas* L and Effects on Spodoptera frugiperda. Quim. Nova, Vol. 35, No. 11, 2218-2221.
37. Saidin NU, Saidin M, Kamarudin SRM, Samsu Z, Muhamad A, Ripin MS, Rejab R, and Sattar MS. (2011) 168 Hours Salt Fog Test. Nuclear Technical Convention, Malaysian Nuclear Agency:1–6
38. Sangeetha M, Rajendran S, Muthumegala TS, and Krishnaveni A (2011) Green corrosion inhibitors-An Overview. ZAŠTITA MATERIJALA 52, broj 1:1–17
39. Sastri VS (2011) Green Corrosion Inhibitors; Theory and Practice:257–288
40. Sastri VS, Ghali E, and Elboudjaini M. (2007) Corrosion Prevention and Protection Practical Solutions.:80–90.
41. Sathiyabama S, Rajendran J, Selvi A. (2006) Methyl orange as corrosion inhibitor for carbon steel in well water. Bull. Electrochemistry 22:363–370
42. Siatou A, Argyropoulos V, Charalambous D, Polikreti K, and Kaminari A. (2007) Testing New Coating Systems for the Long-Term Protection of Copper and Iron Alloy Collections Exposed in Uncontrolled Museum Environment. CSSIM Conference:1–6
43. Tang F, Wang X, Xu, X, and Li, L (2010) Phytic acid doped nanoparticles for green anticorrosion coatings. Colloids Surf. A 369:101–105
44. Usman BJ, Scenini F, Curioni M (2020) Corrosion Testing of Anodized Aerospace Alloys: Comparison Between Immersion and Salt Spray Testing using Electrochemical Impedance Spectroscopy. Journal of the Electrochemical Society 167: 1–16
45. Winnicki M, Baszczuk A, Jasiorski M, and Malachowska A (2017) Corrosion Resistance of Copper Coatings Deposited by Cold Spraying. J Therm Spray Tech 26:1935–1946
46. Zaferani Sh, Sharifi M, Zaarei D, Shishesaz MR (2013) Application of eco-friendly products as corrosion inhibitors for metals in acid pickling processes – A review. J Env Chem Eng 1:652–657